Enhancement of Critical Current Density in MgB2 Bulk Superconductors by Ti Doping

Author:
Zhao, Yong; Feng, Y; Machi, T; Cheng, C; Huang, D; Fudamoto, Y; Koshizuka, N; Murakami, M

Publication details:
Europhysics Letters
v. 57
pp. 437-443
0295-5075 (ISSN)

Publication Date:
2002

Publisher DOI:
http://dx.doi.org/10.1209/epl/i2002-00479-1

EUROPHYSICS LETTERS 1 February 2002

Europhys. Lett., **57** (3), pp. 437–443 (2002)

Enhancement of critical current density in MgB_2 bulk superconductor by Ti doping

Y. Zhao[1,2](*), Y. Feng[1], T. Machi[1], C. H. Cheng[2], D. X. Huang[1], Y. Fudamoto[1], N. Koshizuka[1] and M. Murakami[1]

[1] *Superconductivity Research Laboratory, ISTEC*
1-10-13 Shinonome, Koto-ku, Tokyo 135, Japan
[2] *Superconductivity Research Group, School of Materials Science and Engineering*
University of New South Wales - Sydney, 2052 NSW, Australia

(received 12 July 2001; accepted in final form 12 November 2001)

PACS. 74.60.Jg – Critical currents.
PACS. 74.70.Ad – Metals; alloys and binary compounds (including A15, Laves phases, etc.).
PACS. 74.60.Ge – Flux pinning, flux creep, and flux-line lattice dynamics.

Abstract. – We studied the Ti doping effect on the superconducting properties and microstructure of sintered MgB_2 bulk polycrystals. Using Ti as a sintering assistant, we have fabricated MgB_2 bulk materials consisting of fine 10 nm scale particles and achieved a high J_c of 1 MA/cm^2 in self-field and 3×10^5 A/cm^2 in 1 T at 20 K. The large enhancement of J_c is explained by the excellent connection between grains and the high density of pinning centers served by both grain boundaries and MgO nanoparticles.

The recent discovery of superconductivity in MgB_2 by Akimitsu *et al.* [1] introduces a new and important member to the superconductor family with its relatively high critical temperature ($T_c = 39$ K). MgB_2 is a promising candidate for engineering applications in the temperature range of liquid hydrogen (20 to 30 K) where the conventional superconductors cannot play any role because of low T_c. In addition, unlike the high-temperature superconductors (HTS), MgB_2 has a simple chemical composition and crystal structure, and no weak-link problem at grain boundaries [2, 3], providing a high feasibility to scale up the material to form bulk shapes like wires and tapes. However, the critical current density J_c of MgB_2 bulk materials sintered at ambient pressure is relatively low [3, 4] compared to the conventional A15 compound superconductors, due to a poor connection between grains and the lack of flux pinning centers in the materials. Although high-pressure sintering [5, 6] and proton irradiation [7] have been used to improve the grain connection and flux pinning, respectively, these techniques are not available for manufacturing wires and tapes for large-scale applications. Thus, the fabrication of high-performance MgB_2 bulk materials with industrially feasible techniques is still a challenge to the superconductivity community.

For sintered MgB_2 bulk materials including those prepared under a high pressure of several GPa, the grain size of MgB_2 is usually quite large, ranging from 0.1 to 10 μm [8, 9], making

(*) E-mail: zhao@istec.or.jp

it difficult to form tight packing between grains during the conventional sintering process. Formation of thick grain boundaries of several nanometers or more has been observed even in the samples prepared under a high pressure of 6 GPa [8]. Besides, MgB_4, as an impurity phase in the grain boundary region [8,9], may further loose the connection between the MgB_2 grains due to a large mismatch in crystal structure and lattice constants between the two boride phases. On the other hand, a large grain size leads to a reduction of the effective surface area for the grain boundaries that may be important pinning centers in MgB_2, as observed in Nb_3Sn [10].

Here we present a simple and reliable method to make high-density and high-performance MgB_2 bulk materials at ambient pressure. In our approach, fine Ti powder is used as sintering assistant: with Ti doping, a very thin layer (less than 1 nm) of TiB_2 forms around the MgB_2 particles, decreasing the growth rate of the MgB_2 grains and resulting in a tightly bonded MgB_2 nanoparticle assembly. Due to the improved grain connection, the increased surface area of grain boundaries and a large quantity of fine MgO particles inserted in the MgB_2 nanoparticle assembly, the J_c of MgB_2 bulk samples has been significantly improved, *e.g.*, $1\,\mathrm{MA\,cm^{-2}}$ at 20 K has been achieved in the optimally Ti-doped MgB_2.

A series of Ti-doped MgB_2 samples with an atomic ratio of $Mg : Ti : B = 1 - x : x : 2$ and $0 \leq x \leq 1.0$ were prepared by solid-state reaction at ambient pressure. Mg (99%), Ti (99%) and B (99%) powders were mixed and ground in air for 0.5 to 2 hours. 5% extra Mg powder was added in the starting materials to compensate the loss of Mg due to its evaporation at high temperature. The mixture was pressed into cylinders and placed on a MgO plate. The sintering was carried out in flowing Ar at 800 °C to 900 °C for 1 to 3 h, and then followed by furnace cooling. The crystal structure was investigated by powder X-ray diffraction (XRD) using a MXP18 (MAC Science Co., Ltd) diffractometer with a Cu K_α radiation. The microstructural and compositional analyses were performed by a field emission high-resolution transmission electron microscope (FEHRTEM) equipped with an energy-dispersive X-ray spectroscopy (EDX) system. The DC magnetization was measured using a RF SQUID magnetometer (Quantum Design MPMSR2). The dimensions of the samples used for this study are $0.71 \times 0.83 \times 1.08\,\mathrm{mm^3}$ for pure MgB_2 and $0.41 \times 0.57 \times 0.83\,\mathrm{mm^3}$ for the Ti-doped sample ($x = 0.1$). The field was applied in the direction along the shortest dimension of the sample. J_c values were deduced from the hysteresis loops using the Bean model [11]. The irreversibility field was determined from the closure of hysteresis loops with a criterion of $10^2\,\mathrm{A/cm^2}$. As reported previously [12], the microstructure, diamagnetic response, and J_c of Ti-doped MgB_2 bulk materials vary significantly with doping level, and the optimum doping level has been found at $x = 0.1$.

The temperature dependence of the magnetization for the optimally Ti-doped sample ($x = 0.1$) is shown in fig. 1 as an inset. The sample shows a superconducting transition at $T_c = 37.9$ K with a transition width $\Delta T_c < 1$ K, indicating the uniformity of the phase and good connection between grains. The transitions in zero-field–cooling (ZFC) and field-cooling (FC) processes are significantly separated, which reflects a strong flux trapping in the sample. As compared to the pure MgB_2 sample (*i.e.*, $x = 0$, see also fig. 1) [13], the Ti-doped one exhibits a better diamagnetic response at all temperatures below T_c.

The hysteresis loops at 20 K for the samples with $x = 0$ and 0.1 are displayed in fig. 1. Compared to the pure MgB_2 sample, the Ti-doped sample shows a much wider hysteresis loop and higher irreversibility field at the same temperature. This clearly demonstrates that the pinning force of the MgB_2 bulk materials is significantly enhanced by doping Ti, and the irreversibility behavior is greatly improved as well.

Figure 2 shows the $J_c(H)$ curves for Ti-doped and pure MgB_2 samples at several selected temperatures. At all temperatures examined in this study, the Ti-doped sample exhibits

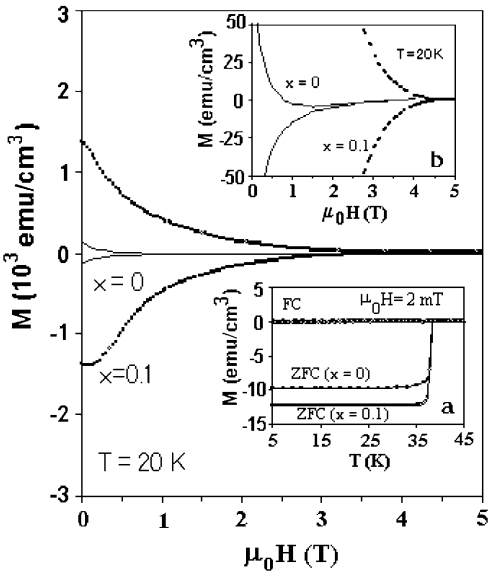

Fig. 1

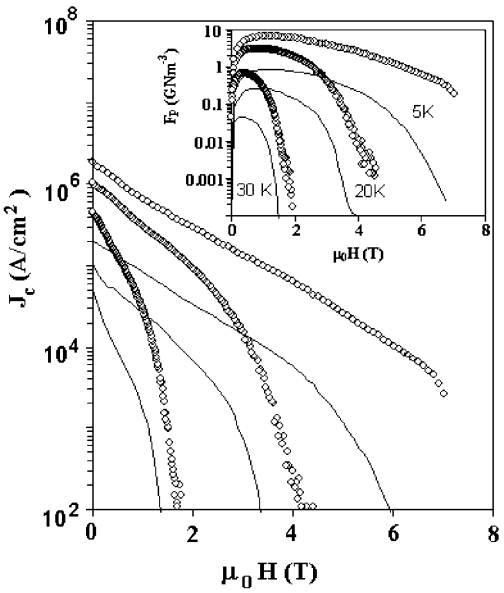

Fig. 2

Fig. 1 – Hysteresis loops for Ti-doped ($x = 0.1$) and pure ($x = 0$) MgB_2 bulk samples measured at 20 K. The inset (a) shows the temperature dependence of the DC magnetization in the field of 2 mT for the same samples in the zero-field–cooling (ZFC) and field-cooling (FC) processes. The inset (b) shows a magnified view of the closure of hysteresis loops.

Fig. 2 – $J_c(H)$ curves measured at 5, 20 and 30 K for Ti-doped MgB_2 with $x = 0.1$ (represented by dots) and pure MgB_2 (represented by solid lines). The inset shows the field dependence of the pinning force density, $F_p = \mu_0 H J_c(H)$, for the same samples.

a higher J_c than the pure one. Some noticeable values of J_c for the Ti-doped sample are summarized as follows. At 5 K, the J_c reaches 2×10^6 A/cm^2 in the self-field, 3×10^5 A/cm^2 in 2 T, and 5×10^4 A/cm^2 in 5 T. At $T = 20$ K, J_c is as high as 1.3×10^6 A/cm^2 in the self-field, 3.1×10^5 A/cm^2 in 1 T, 9.4×10^4 A/cm^2 in 2 T and 1.7×10^4 A/cm^2 in 3 T. All these J_c data are much higher than the best results reported so far for MgB_2 bulk materials including those prepared under high pressure (the typical value of J_c is 2×10^4 A/cm^2 at 20 K and 1 T [5]), proton-irradiated MgB_2 fragments (the typical value of J_c is 2×10^5 A/cm^2 at 20 K and 1 T [7]), and the dense wires (the typical value of J_c is 3×10^4 A/cm^2 at 20 K and 1 T [14]). Besides, the bulk pinning force, $F_p(H) = \mu_0 H J_c(H)$, reaches 7 GN m^{-3} at 5 K (see the inset of fig. 2), which is one order of magnitude higher than that for pure MgB_2 bulk sample, and is close to the pinning force of the established technological superconductors Nb 47 wt% Ti [15] and Nb_3Sn [16], which lie in the range 15–30 GN m^{-3}.

The irreversibility fields $\mu_0 H_{irr}$ for the Ti-doped and pure MgB_2 samples are summarized in fig. 3. The typical irreversibility field $\mu_0 H_{irr}$ for the Ti-doped sample reaches 7 T at 10 K and 4.5 T at 20 K. These data are again much higher than the best result achieved in other MgB_2 bulk samples including those sintered under high pressure [5,6]. The temperature dependence of the irreversibility lines shown in fig. 3 can be fitted by a power law as

$$\mu_0 H_{irr}(T) = \mu_0 H_0 (1 - T/T_c)^m, \tag{1}$$

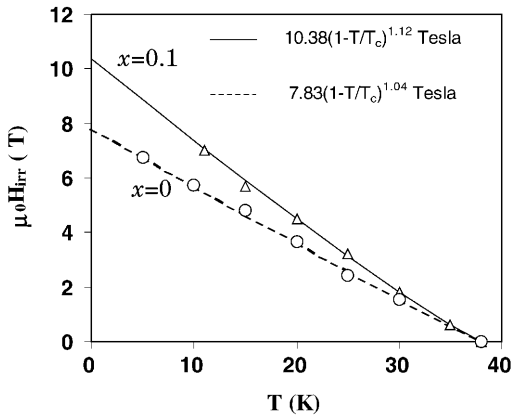

Fig. 3 – Temperature dependence of the irreversibility field for Ti-doped MgB_2 with $x = 0.1$ (denoted by triangles) and pure MgB_2 (denoted by circles). The dashed and solid lines represent the fitting of eq. (1) for the samples with $x = 0$ and $x = 0.1$, respectively.

with $m = 1.04$ and $\mu_0 H_0 = 7.83\,\mathrm{T}$ for the pure MgB_2 sample, and $m = 1.12$ and $\mu_0 H_0 = 10.38\,\mathrm{T}$ for the Ti-doped sample ($x = 0.1$). It can be seen here that the irreversibility field at zero temperature is over 10 T for Ti-doped MgB_2.

The underlying mechanisms for the improvement of J_c and the enhancement of pinning force in the Ti-doped MgB_2 samples can be attributed to two main factors —a strong connection between grains and a very large pinning force.

Figure 4 shows transmission electron micrographs of Ti-doped MgB_2 samples. The samples mainly consist of MgB_2 fine particles with an average size of $\sim 10\,\mathrm{nm}$ and a volume fraction exceeding 90% (see fig. 4a). These nanoparticles are packed tightly with a thin grain boundary of 1 nm or less (see figs. 4b and d). This is in great contrast with other MgB_2 bulk materials prepared under ambient pressure, in which a loose packing of the coarse particles and an amorphous boundary with a thickness of 10 nm or more are often observed [8,9]. The packing of the MgB_2 particles in the Ti-doped sample is even denser than that in the MgB_2 sample synthesized under a high pressure of several GPa, in which the grain size is around several microns and the grain boundary is of several nanometers in thickness [8]. A combination of very thin grain boundaries and extremely tight packing between the particles in the Ti-doped MgB_2 bulk materials leads to extremely high J_c in both low and high fields, as shown in fig. 2.

As shown in fig. 4a, the grain size is about 10 nm, which provides strong grain boundary pinning like Nb_3Sn, for which F_p is inversely proportional to the grain size [10]. In addition, as shown in fig. 4e, a large number of fine MgO particles of 10 to 20 nm in diameter are distributed in the MgB_2 nanoparticle assembly, which may also contribute significantly to the pinning force enhancement. It is probable that the oxygen comes from the slight oxygenation of Mg powder during mixing with B and Ti powders in air. Hence, good grain connection and the introduction of pinning centers have been simultaneously achieved in MgB_2 bulk sample through Ti doping, which is responsible for the high J_c values and the improved irreversibility field. The microstructure of the Ti-doped sample is quite similar to that of the MgB_2 thin films [17], which consists of fine 10 nm scale MgB_2 grains and many MgO fine particles, and reaches an extremely high irreversibility field up to 15 T at 4.2 K.

The mechanism of Ti doping on a microstructure of MgB_2 can be understood with the results of the microstructural and compositional analyses shown in fig. 4. As revealed by the

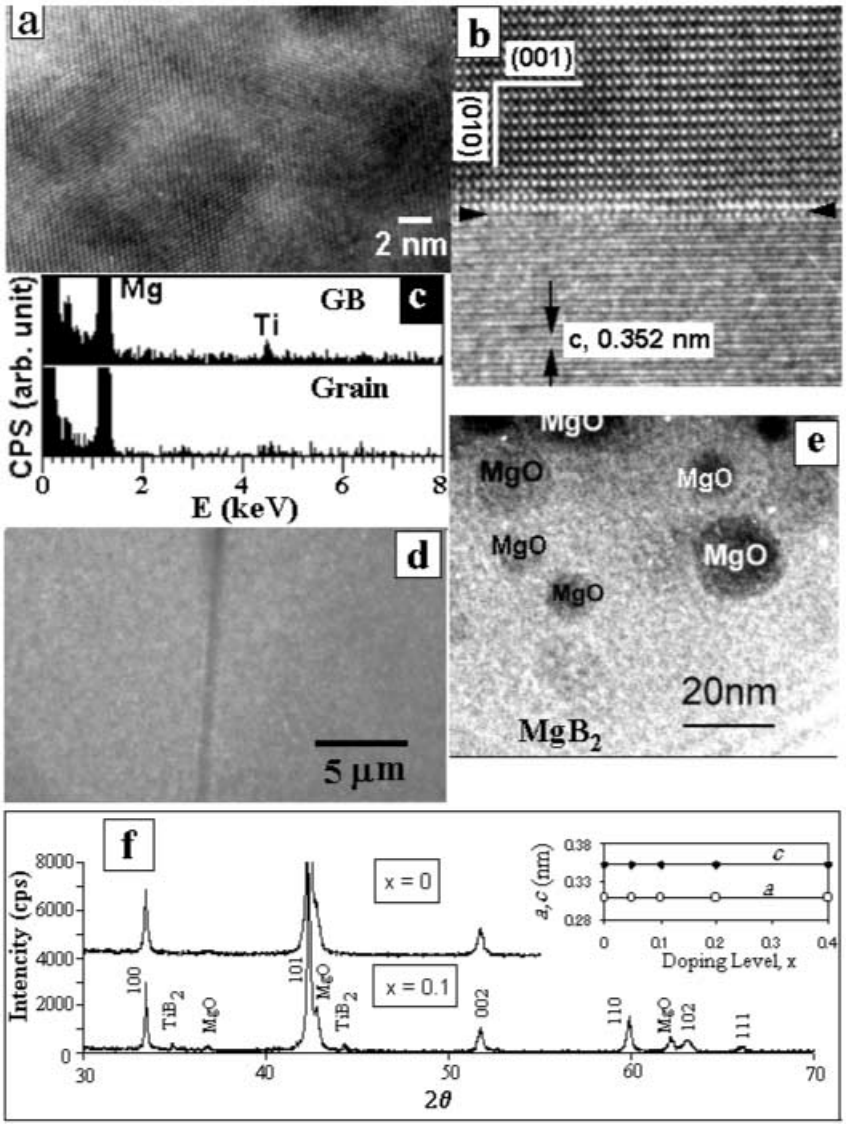

Fig. 4 – a) High-resolution transmission electron microscopy for the Ti-doped sample ($x = 0.1$), which clearly shows that the size of the MgB_2 grains is around 10 nm, packed tightly to each other. About 90% in the volume of the sample is made by these nanoparticles. b) Magnified view of a typical grain boundary (indicated by the black triangles) which shows a very small GB thickness. c) EDX results taken in the regions of the grain boundary (GB) and grain shown in panel b). The EDX results demonstrate that Ti only exists in the grain boundary region. d) TEM image for grain boundary between particles of a size around 20 nm. This grain boundary is thicker than that shown in panel b), however, the size is still smaller than 1 nm. About 10% in volume of the sample is made from this kind of nanoparticles. e) This TEM image shows a high density of MgO particles, with a size between 10 to 20 nm, inserted in the MgB_2 nanoparticle assembly. f) XRD patterns for Ti-doped ($x = 0.1$) and pure MgB_2 ($x = 0$) in which TiB_2 and MgO are presented as the second phases. The inset shows that the lattice constants do not change with the Ti doping level ($0 \leq x \leq 0.4$).

EDX analysis (see fig. 4c), the Ti element was only found at the grain boundary rather than inside the MgB_2 grains. The EDX analysis was carried out with an electron beam of 1 nm in diameter in the regions of grain boundary and grain, and thus provides clear information of the local composition around the grain boundary. The EDX results are also consistent with the XRD analysis which reveals that the Ti doping does not change the lattice constants of MgB_2 but forms TiB_2 as impurity phase (see inset of fig. 4f). A comprehensive analysis based on these results suggests that Ti does not occupy atomic sites in the crystal structure, and it rather works as a sintering assistant. With Ti doping, a very thin layer (less than 1 nm because the total thickness of grain boundary is less than 1 nm) of TiB_2 forms around the MgB_2 particles, which may decrease the growth rate of the MgB_2 grains and result in the formation of very fine MgB_2 particles. Because no MgB_4 was observed at grain boundaries for Ti-doped MgB_2, it is reasonable to further postulate that the formation of TiB_2 may also prevent the formation of MgB_4 which usually stays in the grain boundaries of MgB_2 [8,9] and causes a loose connection between grains due to its large mismatch in the crystal structures and the lattice constants with MgB_2 (which has a hexagonal structure with $a = 0.3086$ nm and $c = 0.3524$ nm [1], whereas MgB_4 has an orthorhombic structure with $a = 0.5464$ nm, $b = 0.7472$ nm and $c = 0.4428$ nm). In contrast to MgB_4, the TiB_2 has a much better bonding with MgB_2 due to the same crystal structure and very close lattice constants ($a = 0.3030$ nm and $c = 03230$ nm). The TiB_2 layer does not cause any weak-link effect, as confirmed by the very high J_c in both low and high fields (temperatures), due to its very small thickness.

As shown in our previous report [12], the microstructure of Ti-doped MgB_2 including the grain size of MgB_2 and the thickness of the grain boundaries can be controlled by changing the doping level and the sintering conditions. Increasing the doping level often results in the formation of a thick grain boundary which weakens the grain connection and thus decreases the J_c. Typically, as the doping level increases to $x = 0.4$, the shielding current is decreased by four orders of magnitude, indicating a dramatic weak-link effect. On the other hand, prolonging the sintering time may result in an increase of the MgB_2 grain size and thus degrade the grain boundary pinning effect. For example, the sample with $x = 0.1$ sintered at 900 °C for 5 h with an intermediate grinding exhibits a significant drop of J_c in a high field (J_c at 20 K in 3 T drops by more than one order of magnitude). Indeed, the technique developed in this study is a flexible method to tune the dimensions of the particles and the grain boundaries in MgB_2.

In summary, we have demonstrated a simple and reliable method to control the microstructure of MgB_2 by using Ti as a sintering assistant. MgB_2 bulk materials consisting of fine 10 nm scale particles have been fabricated by means of this technique, and the high J_c of 1 MA/cm^2 in self-field and 3×10^5 A/cm^2 in 1 T at 20 K have been achieved. The large enhancement of J_c is explained by the excellent connection between grains and the high density of pinning centers served by both grain boundaries and MgO nanoparticles.

* * *

This work was supported in part by New Energy and Industrial Technology Development Organization (NEDO), Japan.

REFERENCES

[1] Nagamatsu J., Nakagawa N., Muranaka T., Zenitani Y. and Akimitsu J., *Nature*, **410** (2001) 63.
[2] Larbarlestier D. C., Rikel M. O., Cooley M. D. *et al.*, *Nature*, **410** (2001) 186.

[3] Bugoslavsky Y., Perkins G. K., Qi X., Cohen L. F. and Caplin A. D., *Nature*, **410** (2001) 563.
[4] Finnemore D. K., Ostenson J. E., Bud'ko S. L. *et al.*, *Phys. Rev. Lett.*, **86** (2001) 2420.
[5] Takano Y., Takeya H., Fuji H. *et al.*, *Appl. Phys. Lett.*, **78** (2001) 2914.
[6] Wen H. H., Li S. L., Zhao Z. W. *et al.*, *Chin. Phys. Lett.*, **18** (2001) 816.
[7] Bugoslavsky Y., Cohen L. F., Perkins G. K. *et al.*, *Nature*, **411** (2001) 561.
[8] Li J. Q., Li L., Zhou Y. Q. *et al.*, *Chin. Phys. Lett.*, **18** (2001) 680.
[9] Zhu Y., Wu L., Volkov V. *et al.*, *Physica C*, **356** (2001) 239.
[10] Campbell A. M. and Evetts J. E., *Adv. Phys.*, **21** (1972) 199.
[11] Bean C. P., *Rev. Mod. Phys.*, **36** (1964) 31.
[12] Zhao Y. *et al.*, *Appl. Phys. Lett.*, **79** (2001) 1154.
[13] The optimal conditions for making the pure MgB_2 sample (*i.e.*, $x = 0$) is different from those for $x = 0.1$. The sample of $x = 0$ was prepared at 750 °C for 2 h in Ar atmosphere.
[14] Jin S., Mavoori H. and van Dover R. B., *Nature*, **411** (2001) 563.
[15] Lee P. J., in *Wiley Encyclopedia of Electronics Engineering*, edited by Webster J. G., Vol. **21** (Wiley, New York) 1999, p. 75.
[16] Smathers D. B., in *Metals Handbook*, *Properties and Selection: Nonferros Alloys and Specia-Purpose Materials 1060*, 10th edition, Vol. **2** (ASM Intl) 1990.
[17] Eorn C. B., Lee M. K., Choi J. H. *et al.*, *Nature*, **411** (2001) 558.